論文

Modeling and Validation of Induced Strain Actuation of Composite Coupled Plates

Chang-Ho Hong*

복합재료 연성판의 유기변형률제어 모델링과 검증

홍창호*

초 록

유기변형률제어를 가지는 복합재료연성판의 해석을 위하여 적합변형을 가지는 판유한요소모델을 정식화하고 이를 등방성 및 이방성 외팔보의 실험데이터와 비교하여 검증하였다. 제어기는 기저층판과 완전히 결합되는 부가적인 얇은판으로 간주되었으며 정식화는 수정된 고전층판이론에 근거하여 수행되었다. 이방성 판모델은 임의의 크기의 압전제어기가 임의의 위치에 표면부착 또는 심겨져 있는 것으로 하였다. 인장-비틈과 굽힘-비틈연성을 가지는 복합재료판이 제작되고 시험되었다. 압전세라믹은 판의 지지단 쪽 표면의 상하에 이열로 부착되었다. 정적시험은 기계적하중과 유기변형률제어를 사용하여 수행되었으며 측정치는 굽힘 및 비틈분포에 대한 예측치와 비교되었다. 인장-비틈 연성판에서는 압전제어의 인장변형률에 의한 유기비틈에 대하여 예측치와 측정치가 매우 잘 맞고 있다. 굽힘-비틈이 강한 연성판에서는 압전제어의 굽힘변형률에 의한 유기비틈이 측정치와 경향은 잘 맞으나 크기에서는 20% 정도 낮게 예측되고 있다. 굽힘-비틈이 약한 연성판에서는 예측된 유기비틈이 측정치와 매우 잘 맞고 있다. 모델링과 검증결과는 판의 형상제어 분야에서 압전제어기의 활용가능성을 보여주었다.

ABSTRACT

A consistent plate finite element model is formulated for coupled composite plates with induced strain actuation, and validated with test data obtained from cantilevered isotropic and anisotropic plates. Actuators are modeled as additional plies fully integrated into substrate laminae, and the formulation is based on modified thin classical laminated plate theory. The analysis is formulated for a generic anisotropic plate with a number of piezo actuators of arbitrary size, surface-bonded or embedded at arbitrary locations. Composite plates with extension-twist and bending-twist couplings were built and tested. Two rows of piezoceramic elements are surface mounted on both top and bottom surfaces near the root. Static tests are carried out using induced strain actuation, and mechanical loading and measured data are correlated with predictions for bending and twist distributions. For an extension-twist coupled plate, the agreement between predicted and measured induced twist due to extensional strain with piezo actuation is excellent. For the strongly bending-twist coupled composite plate, the predicted induced twist due to bending strain with piezo

*충남대학교 공과대학 항공우주공학과

actuation agreed well in trends but magnitudes were underpredicted by a maximum of 20% from measured values. For the weakly bending-twist coupled composite plate, the predicted induced twist angle agreed extremely well with measured data. The modeling and validation results show the useability of the piezo actuation in the field of plate shape control.

1. Introduction

Adaptive structures with embedded or surface-mounted strain-induced actuators are evolving in applications to various physical systems to actively control vibration, noise, aeroelastic stability, damping, shape and stress distribution. Physical systems range from spacecraft, fixed-wing and rotary-wing aircraft, to automotive and other ground systems. One of the basic elements of adaptive structures is a thin composite plate with such distributed induced strain actuators as piezoceramic actuators. With tailored anisotropic plates, induced strain actuation can be used to control the extension, bending and twisting of the structure.

The state-of-the-art on modeling of composite laminated plates, with induced strain actuation and systematic validation with test data, is limited. Most analyses assume piezo actuators as additional plies fully integrated with laminae of the substrate, and use thin classical laminated plate theory (CLPT) to develop formulations. Crawley and Lazarus [1] developed a simple Rayleigh-Ritz analysis of isotropic and anisotropic plates with induced strain actuation, and validated it with test data they obtained by testing of cantilevered isotropic and composite plates with piezoelectric actuators (surface-mounted entirely on both surfaces). Nonlinear piezoelectric constants (d31 and d32) were measured experimentally and included in the analysis using an iterative procedure. Results demonstrated the validity of the model for some selected plate configurations as well as the potential of using induced strain actuation for shape control of elastic structures. Lee [2] also developed a thin laminated composite plate formulation with piezoelectric laminae using linear actuation characteristics. A limited validation study was carried out with data obtained from the testing of a thin composite plate actuated with piezoelectric polymer film (PVDF and PVF2). Wang and Rogers [3] applied classical laminated plate theory to determine the equivalent force and moment induced by finite-length piezo actuators attached to a laminate. Using linear piezo characteristics, they showed that induced inplane forces and line moments along four edges of the actuator cause bending and extension of the plate. The refined composite plate theories with induced strain actuation were developed by Mitchell and Reddy [4], but were not substantiated with test data or results from other theories. Ha, Keilers and Chang [5] developed a linear finite element analysis of a laminated composite plate containing distributed piezoceramics. An eight-node three-dimensional composite brick element was incorperated into the analysis. Predicted induced deflections from surface-bonded piezo actuators were compared with test data from Ref. [1]. The agreement was less than satisfactory, in particular for induced twist. Shah, Chan and Joshi [6] developed a linear finite element analysis of laminated plates with piezoelectric plies. A nine-node isoparametric quadrilateral element was implemented in the analysis. No validation studies were carried out. The analyses use linear piezoelectric characteristics and are not validated systematically with test data. Lee and Saravanos[7] also developed a similar finite element analysis of laminated plates with piezoelectric elements as Ref. [5] under thermal loading. A bilinear four-node plate element was used. Results were obtained using linear piezoelectric constants, and only a part of

results was compared with the analytic result of Ref. [5]. The intent of the present paper is to address these two important issues - nonlinear piezoelectric characteristics and validation with test data.

The present paper develops a consistent finite element laminated plate analysis for a thin coupled composite plate with piezoelectric actuators placed at arbitrary locations. The formulation uses direct nonlinear free strain characteristics of actuators that are obtained by polynomial fitting to the test data. Systematic static tests are carried out on thin aluminum, and coupled bending-twist and extension-twist graphite/epoxy plates with surface-mounted piezoceramics for part of the plate. Test data are used for validation of the analysis.

2. Analytical Modeling

The consistent plate model is formulated for the analysis of a laminated plate bonded with piezoceramic actuators. The assumptions made are: (1) actuators and substrate are integrated as plies of a laminated plate, (2) consistent deformation exists in the actuators and substrate, and (3) laminate plate theory is adopted, but transverse shear deformation is allowed (the line originally normal to the mid-plane of the plate becomes inclined to the mid-plane after bending deflection). Assumptions (1) and (2) implies a perfect bonded condition between actuators and substrate. This is a generic thin plate analysis for anisotropic plates with a number of actuators of arbitrary size, surface-bonded or embedded and placed at arbitrary locations. Based upon above assumptions, the strains in the plate are

$$\varepsilon=\begin{Bmatrix}\varepsilon^0\\ z\kappa\\ \gamma\end{Bmatrix} \quad \cdots\cdots (1)$$

$$\varepsilon^0=\begin{Bmatrix}\varepsilon_x^0\\ \varepsilon_y^0\\ \gamma_{xy}^0\end{Bmatrix},\ \kappa=\begin{Bmatrix}\kappa_x\\ \kappa_y\\ \kappa_{xy}\end{Bmatrix}=\begin{Bmatrix}\dfrac{\partial\theta_x}{\partial x}\\ \dfrac{\partial\theta_y}{\partial y}\\ \dfrac{\partial\theta_x}{\partial y}+\dfrac{\partial\theta_y}{\partial x}\end{Bmatrix},$$

$$\kappa=\begin{Bmatrix}\theta_x-\dfrac{\partial\theta_x}{\partial x}\\ \theta_y-\dfrac{\partial\theta_y}{\partial y}\end{Bmatrix} \quad \cdots\cdots (2)$$

where ε_x^0, ε_y^0 and are mid-plane strains, and θ_x and θ_y are plate rotation angles from z, the reference coordinate axis, normal to the mid-plane of the plate before bending.

The constitutive relation for any ply of a laminated plate is

$$\sigma=Q(\varepsilon-\Lambda) \quad \cdots\cdots (3)$$

where

$$\sigma^0=\begin{Bmatrix}\sigma_x\\ \sigma_y\\ \tau_{xy}\\ \tau_{xz}\\ \tau_{yz}\end{Bmatrix},\quad \Lambda=\begin{Bmatrix}\Lambda_x\\ \Lambda_y\\ 0\\ 0\\ 0\end{Bmatrix} \quad \cdots\cdots (4)$$

and **Q** is the transformed reduced stiffness matrix of the ply. Here, the substrate is assumed to consist of anisotropic laminae and the actuators are isotropic laminae. In the induced actuation strain vector Λ, there is no shear strain component in it.

3. Finite Element Formulation

The total potential energy of the system is given by

$$\Pi=U-W \quad \cdots\cdots (5)$$

where U is the strain energy and W is the work done by the external forces. U can be expressed as

$$U=\frac{1}{2}\int_V \varepsilon^T Q\varepsilon dV-\int_V \varepsilon^T Q\Lambda dV \quad \cdots\cdots (6)$$

An eight-node plate element is used to model the laminated plate. The plate displacement vector **u** has five degrees of freedom and is given as

$$\mathbf{u}=\begin{Bmatrix} u \\ v \\ w \\ \theta_x \\ \theta_y \end{Bmatrix} \quad \cdots\cdots (7)$$

For the finite element discretization, **u** is expressed using shape function matrix ϕ[8] and nodal displacement vector **d** as

$$\mathbf{u}=\phi\mathbf{d} \quad \cdots\cdots (8)$$

The generalized strain-displacement relation for the plate bending element allowing inplane displacements can be written as

$$\varepsilon=\mathbf{Bu} \quad \cdots\cdots (9)$$

where is **B** the strain-displacement matrix and $\mathbf{B}_i$, **B** of the i^{th} node, is given as

$$\mathrm{Bi}=\begin{bmatrix} \frac{\partial\phi_i}{\partial x} & 0 & \frac{\partial\phi_i}{\partial y} & 0 & 0 & 0 & 0 & 0 \\ 0 & \frac{\partial\phi_i}{\partial y} & \frac{\partial\phi_i}{\partial x} & 0 & 0 & 0 & 0 & 0 \\ 0 & 0 & 0 & 0 & 0 & -\frac{\partial\phi_i}{\partial y} & \frac{\partial\phi_i}{\partial x} & \\ 0 & 0 & 0 & \frac{\partial\phi_i}{\partial x} & 0 & \frac{\partial\phi_i}{\partial y} & 0 & \phi_i \\ 0 & 0 & 0 & 0 & \frac{\partial\phi_i}{\partial y} & \frac{\partial\phi_i}{\partial x} & \phi_i & 0 \end{bmatrix} \quad \cdots (10)$$

where ϕ_i is the shape function of the i^{th} node.

A selectively reduced integration scheme is used to eliminate locking effects. Using the above equations and applying the principle of virtual work, the finite element formulation can be written as

$$\mathbf{K}^e\mathbf{d}^e=\mathbf{P}_\Lambda^e+\mathbf{F}^e \quad \cdots\cdots (11)$$

where $\mathbf{K}^e$, $\mathbf{P}_\Lambda^e$ and $\mathbf{F}^e$ are the element stiffness matrix, actuation load vector, and external load vector, respectively. These are expressed as

$$\mathbf{K}^e=\int_V \mathbf{B}^T\mathbf{Q}\mathbf{B}dV$$

$$\mathbf{P}_\Lambda^e=\int_V \mathbf{B}^T\mathbf{Q}\Lambda dV \quad \cdots\cdots (12)$$

$$\mathbf{F}^e=\int_V \phi^T\mathbf{f}dS$$

where ϕ is the shape function matrix, and **f** is the external applied nodal load vector.

4. Experiment

Free strain tests were carried out on piezo elements ($2.54cm\times5.08cm\times.254cm$) to determine strain at several voltages. Then a polynomial curve fitting was made to the test data (Fig. 1). In Fig. 1, the induced strains in each orthogonal direction were represented as

$$\Lambda=0.2643\mathrm{E}+0.00028\mathrm{E}^2 \quad \cdots\cdots (13)$$

where E is the applied electric field, *V/mm*.

Aluminum and composite plates of rectangular size ($39.4cm$ by $15.2cm$) were manufactured. Graphite/epoxy plates with bending-twist, and extension-twist coupling were built, each consisting of six plies. Table 1 shows the material properties of piezoceramic (PZT-5H), aluminum, and graphite/epoxy. The PZT-5H was recommended in Ref. [9] as having a high d31 constant, the ratio of free strain to electric field - in the linear region, and a high stiffness. Table 2 shows the layup of composite plates. To achieve a cantilevered condition, a part of plate length ($10.2cm$) is supported

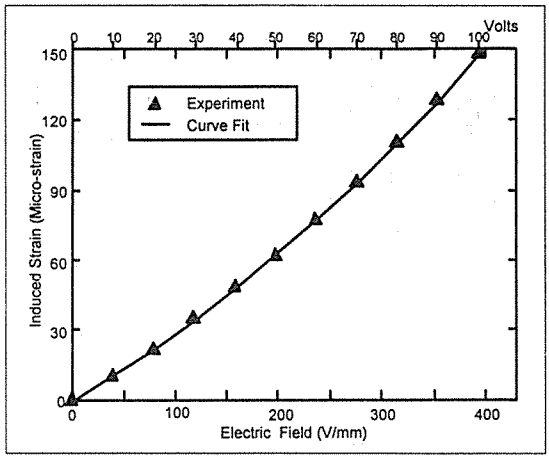

Fig. 1. Free induced strain of piezo element (PZT-5H), Experimental measurement and polynomial curve fitting

Table 1. The material properties of piezoceramic (PZT-5H), aluminum and graphite/epoxy (AS4)

Piezoceramic (PZT-5H)	E=63.0GPa ν=0.3
Aluminum	E=70.0 GPa ν=0.3
Gaphite/Epoxy (AS4)	E_L=143.0 GPa E_T=9.7GPa G_{LT}=6.0GPa ν_{LT}=0.42

with thick aluminum bars, leaving an effective plate span of 29.2*cm*. The 40% root-end of the plate is surface-bonded with 10 equally-spaced actuators (2.54*cm*×5.08*cm*×.254*cm*) on either surface.

Two rows of piezoceramic elements were bonded symmetrically on both the top and bottom surfaces of the aluminum and composite plates. The composite plates were sanded to expose fibers. The aluminum and composite plates acted directly as a common electrode for piezoceramic elements. The resistance of the composite plate was about 30 ohm, much higher than that of aluminum, but there was no measurable heat generation during the static tests. The cantilevered aluminum plate was tested first to verify its induced strain performance. In addition to piezo actuation, an external load of 40 grams mass was applied at the tip of

Table 2. The properties of aluminum and composite Plates

Aluminum	t=0.76mm
Graphite/Epoxy : $[+45_3/-45_3]$	Extension-Twist Coupling t=1.04*mm*
Graphite/Epoxy : $[+30_2/0]_s$	Bending-Twist Coupling t=0.81*mm*
Graphite/Epoxy : $[0/\pm45_3]$	Bending-Twist Coupling t=0.79*mm*

plate. Longitudinal and lateral slopes and twist with tip load and actuation were obtained respectively. To avoid possible creep phenomena, the application of voltages to the desired level was done as quickly as possible. As expected, the creep behavior of piezoceramics was not noticeable under mechanical loading.

Slope angles were measured at discrete locations along the plate span using a laser-optic system ; 60.8, 91, 116.6, 136, 178, 245, 268, and 292*mm* from the root. In the laser-optic system, slope angles, θ, can be obtained using $\theta=d/2L$, where d is the translated distance of the reflected laser beam on the screen and L is the distance between the specimen and the screen. In the test, L was set to be 6.9*m* so as for d to be less than 0.4*m*, giving the most approximated measured values. Fig. 2 shows the arrangement of the 10 actuator elements on each surface, and also locations of mirrors. Bending actuation was applied to the aluminum and the bending-twist coupled plates. For the aluminum plate, longitudinal slopes were measured at mid-chord, while lateral slopes were measured at the side edge. For bending-twist coupled plates, both longitudinal slopes and twist angles were measured at mid-chord. For the extension-twist coupled plate, where actuation was in extension, only twist angles were mea-

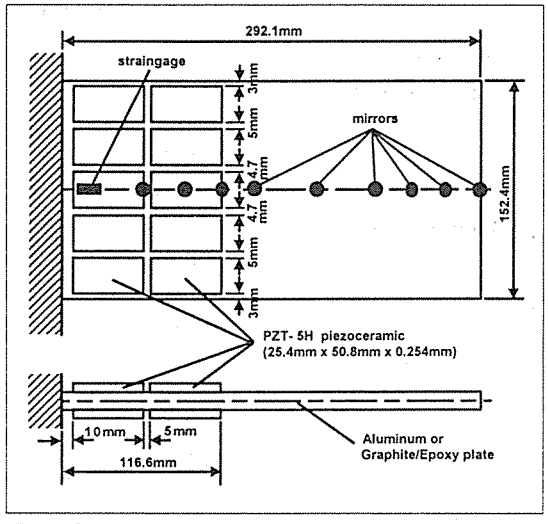

Fig. 2. Cantilevered plate with surface mounted piezoceramics

sured. For each plate, results of finite element analysis due to tip loading were verified with measured values to validate the basic element analysis. Then, similar tests were carried out with the piezo-actuation and data were used to validate modeling of composite plates with induced strain actuation.

5. Results and Discussion

For plate analysis, 198 rectangular finite elements(11 by 18) involving 3265 degrees of freedom are used (Fig. 3).

Fig. 4 shows the longitudinal bending slope distribution at mid-chord of an aluminum plate due to a mechanical load of 40 grams at the tip. . Both predicted results and measured data are presented. The correlation appears very good for this uncoupled plate. The piezo-actuators are attached up to 40% of the plate length from the root resulting in a sudden change of slope distribution at the longitudinal station of 120 *mm*. This change can be attributed to the reduction of effective plate stiffness (absence of stiffness augmentation due to piezos) beyond this station. Fig. 5 presents the

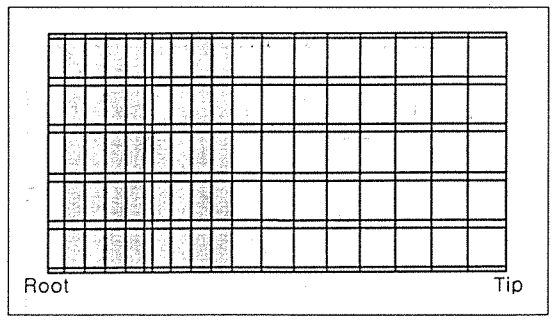

Fig. 3. Finite element modeling of the cantilever plate showing element distribution. Shaded areas represent mounted piezoceramics

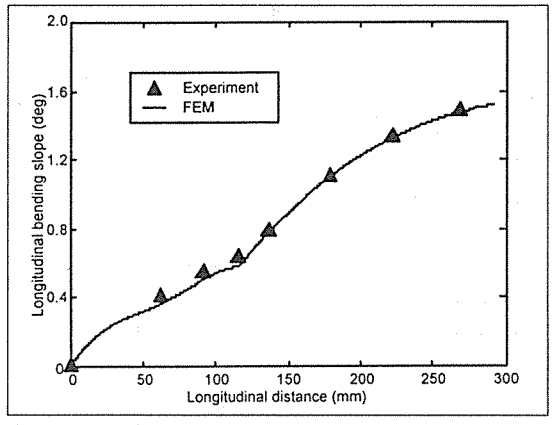

Fig. 4. Longitudinal bending slope at mid-chord of an aluminum plate due to a mechanical load of 40 grams at tip

longitudinal bending slope of the aluminum plate due to bending actuation with piezoceramics. Piezoceramic elements on the top and bottom surfaces are respectively excited by positive and negative potential of 100 volts. The bending slope increases up to 40% in length and then a slight reduction takes place beyond this length. Predictions agree extremely well with test data.

Fig. 6 presents finite element results of longitudinal bending slopes of an aluminum plate due to piezo excitation at 100 volts using linear and nonlinear piezoelectric constants for comparison purpose. The plot using curve-fit data in Fig. 6 is identical with the one by FEM in Fig. 5. The values using nonlinear constant are 42% higher than those using linear constant. The big differences

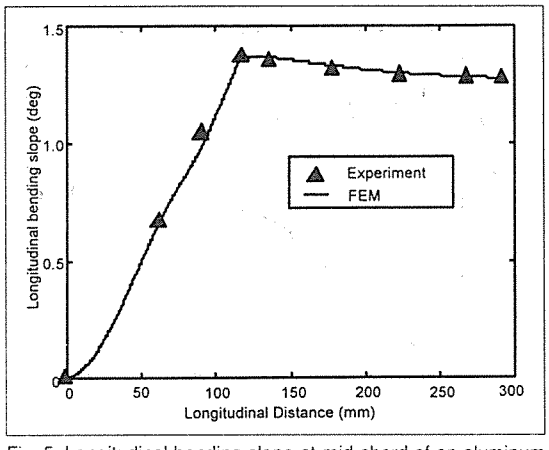

Fig. 5. Longitudinal bending slope at mid-chord of an aluminum plate due to piezo excitation at 100 volts

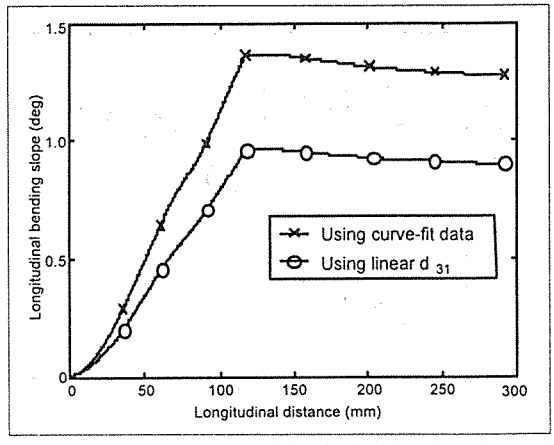

Fig. 6. Finite element results of longitudinal bending slopes at mid-chord of an aluminum plate due to piezo excitation at 100 volts using linear and nonlinear piezoelectric constants

between two plots in Fig. 6 clearly shows the importance of the nonlinear piezoelectric characteristics. The nonlinear characteristics of piezoceramic actuators are used as an input data for the load vector and hence do not require an iterative procedure. This is a key difference from other analysis [1].

Fig. 7 presents the lateral bending slope distribution at the side-edge for this aluminum plate. The lateral bending slope increases up to perhaps 40% in length and then gradually falls to a very small value at the tip. Again, the correlation between predicted and measured values is quite good.

Fig. 8 and Fig. 9 present results for an antisymmetric layup graphite/epoxy plate. This causes an extension-twist coupling. An axial load, in addition to stretching, will also cause twisting of the plate and the bending is uncoupled. Fig. 8 shows longitudinal bending slopes due to a mechanical load of 40 grams at the tip. The slope increases towards the tip and again there is a sudden change at 40% in length. Predictions agree satisfactorily except near the tip where calculated values are higher than measured values by about 10 %. Fig. 9 presents the twist distribution for this plate due to axial actuation with piezos. For this set-up, the same voltage of 100 volts is applied to both top and bottom piezoceramics. Because of extension-

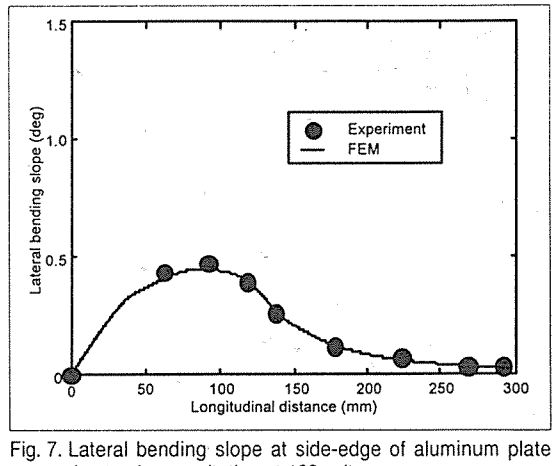

Fig. 7. Lateral bending slope at side-edge of aluminum plate due to piezo excitation at 100 volt

twist coupling, a longitudinal strain will induce twisting of the plate. Predictions of twist agree extremely well with the test data. Since the axial strain stops at 40% length, there is almost no change of induced-twist beyond 40% length.

Fig. 10 to Fig. 13 present results for symmetric layup graphite/epoxy plates. This layup causes a bending-twist coupling. An induced bending actuation will also cause twisting of the plate and the extension remains uncoupled. Fig. 10 and Fig. 11 are for $[+30_2/-0]_s$ plate, where bending-twist coupling is designed to be strong, whereas Fig. 12

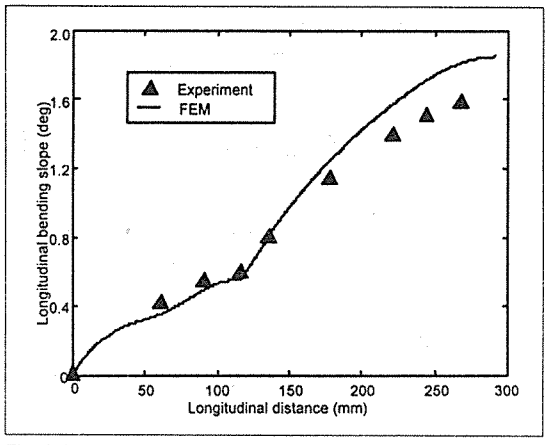

Fig. 8. Longitudinal bending slope at mid-chord of an extension-twist coupled $[+45_3/-45_3]$ graphite/epoxy plate due to a mechanical load of 40 grams at tip

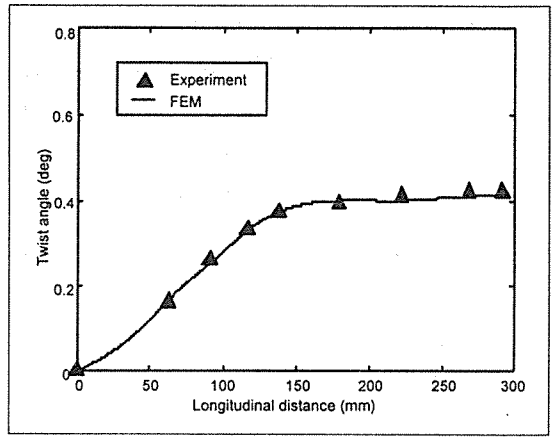

Fig. 9. Twist distribution at mid-chord of an extension-twist coupled $[+45_3/-45_3]$ graphite/epoxy plate due to piezo excitation at 100 volts

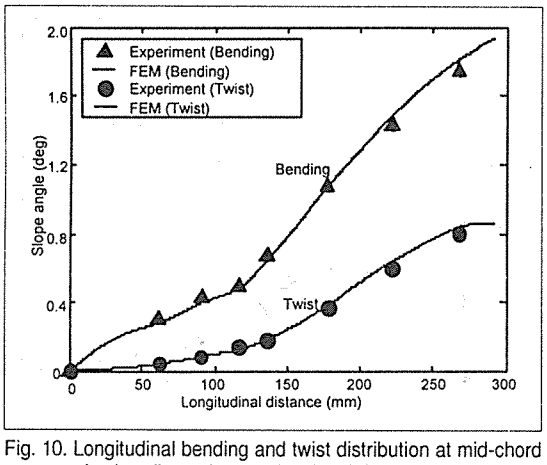

Fig. 10. Longitudinal bending and twist distribution at mid-chord of a bending-twist coupled $[+30_2/-0]_s$ graphite/epoxy plate due to a mechanical load of 40 grams at tip

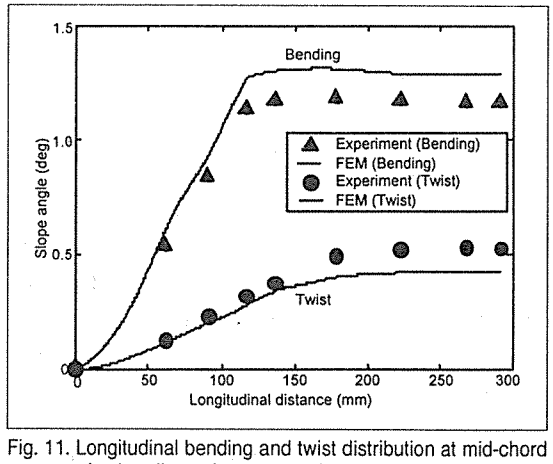

Fig. 11. Longitudinal bending and twist distribution at mid-chord of a bending-twist coupled $[+30_2/-0]_s$ graphite/epoxy plate due to piezo excitation at 100 volts.

and Fig. 13 are for $[0/\pm45]_s$ plate, where bending-twist coupling is designed to be weak.

Fig. 10 shows the longitudinal bending and twist distributions for the strongly coupled plate due to a mechanical load of 40 grams at the tip. Predictions for both bending slope and twist angle are very good. Fig. 11 presents the longitudinal bending slopes and twist distributions for this plate due to induced bending actuation. For this case, opposite potential is applied to the top and bottom piezoceramic actuators. The calculated longitudinal bending slope is somewhat overpredicted from measured values, more so towards the tip where deviations are less then 11%. Predictions for twist angles are good upto around 50% length, but beyond this, are lower than measured values by as much as 20%. Overall predictions are satisfactory and trends are predicted well.

Fig. 12 shows the longitudinal bending and twist distributions for the weakly coupled plate due to a mechanical tip load of 40 grams. Predictions for the bending slopes are very good except

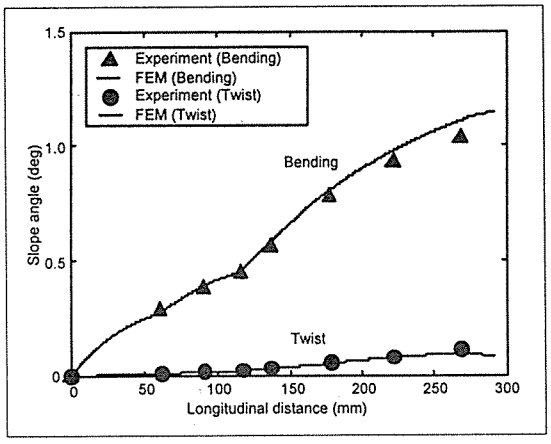

Fig. 12. Longitudinal bending and twist distribution at mid-chord of a bending-twist coupled $[0/\pm45]_s$ graphite/epoxy plate due to a mechanical load of 40 grams at tip

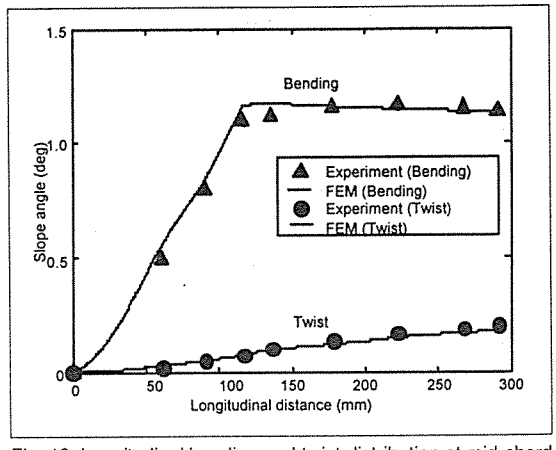

Fig. 13. Longitudinal bending and twist distribution at mid-chord of a bending-twist coupled $[0/\pm45]_s$ graphite/epoxy plate due to piezo excitation at 100 volts

near the tip. Predictions for the twist angle agree very well with test data. Fig. 13 shows longitudinal bending and twist distributions for this plate due to induced bending actuation with an excitation of 100 volts. Predictions for both bending slope and twist angle are quite good.

6. Conclusions

Analysis of thin coupled composite plates with induced strain actuation due to piezoceramics is developed using plate finite element discretization. Aluminum and bending-twist and extension-twist graphite/epoxy plates were built with surface-mounted piezoceramics on both surfaces for part of the plate. Measured slopes and twist distributions were correlated with predictions. For an aluminum plate, the predicted longitudinal slopes due to an induced field of 100 volts agreed extremely well with test data. For an extension-twist coupled plate, the agreement between predicted and measured induced twist due to extensional strain with piezo actuation was excellent. For the strongly bending-twist coupled composite plate, the predicted induced twist due to bending strain with piezo actuation agreed well in trends but magnitudes were underpredicted by a maximum of 20% from measured values. For the weakly bending-twist coupled composite plate, the predicted induced twist angle agreed extremely well with measured data. From these results, the following conclusions are drawn.

1) The present finite element modeling is capable of predicting the response of the composite coupling plates with piezoelectric actuation.

2) The use of nonlinear piezoelectric constants is verified by the excellent agreements between test and predicted data. Also the use of an iterative procedure suggested in Ref. [1] for the calculation of the load vector is found to be not necessary.

3) For the strongly bending-twist coupled plate, the bending to twist coupling ratio of the test is much higher than that of the prediction. The test results shown represent the repeated observation of the different test specimen. This interesting behavior requires further validation study.

4) Finally, the modeling and validation results show the useabilty of the piezoelectric actuation in the field of plate shape control.

Acknowledgements

This research work was carried out while the author stayed at the Alfred Gessow Rotorcraft center, Department of Aerospace Engineering, University of Maryland as a visiting professor. The author express his sincere gratitude to Prof. Chopra for the stimulating present work and his valuable suggestions and comments in the preparation of the manuscript.

References

1. Crawley, E.F. and Lazarus, K.B., "Induced Strain Actuation of Isotropic and Anisotropic Plates", AIAA Journal, Vol. 29, No. 6, 1991, pp. 944-951.

2. Lee, C.K., "Piezoelectric Laminates: Theory and Experiments for Distributed Sensors and Actuators", Intelligent Structural Systems, Ed. Tzou, H.S. and Anderson, G.L., Kulwer Academic Publishers, 1992, pp. 75-168.

3. Wang, B.T. and Rogers, C.A., "Laminate Plate Theory for Spatially Distributed Induced Strain Actuators", Journal of Composite Materials, Vol. 25, No. 4, 1991, pp. 433-452.

4. Mitchell, J.A. and Reddy, J.N., "A Refined Hybrid Plate Theory for Composite Laminates of Piezoelectric Laminae", International Journal of Solids and Structures, Vol. 32, No. 16, 1995, pp. 2345-2367.

5. Ha, S.K., Keilers, C., and Chang, F.K., "Finite Element Analysis of Composite Structures Containing Distributed Piezoelectric Sensors and Actuators", AIAA Journal, Vol. 30, No. 3, 1992, pp. 772-780.

6. Shah, D.K., Chan, W.S., and Joshi, S.P., "Finite Element Analysis of Plates with Piezoelectric Layers", Proceeding of the AIAA/ASME/ASCE/AHS/ASC 34th Structures, Structural Dynamics, and Materials Conference, La Jolla, California, April 19-22, 1993, pp. 3189-3197.

7. Lee, H. J. and Saravanos, D. A., "Active Compensation of Thermally Induced Bending and Twisting in Piezoceramic Composite Plates", Proceeding of the AIAA/ASME/ASCE/AHS/ASC 37th Structures, Structural Dynamics, and Materials Conference, Salt Lake City, Utah, April 18-19, 1996, pp. 120-130.

8. Hinton, E. and Owen, D. R. J., " Finite Element Programming", ACADEMIC PRESS INC. (LONDON) LTD, 1979.

9. Bernhard, A. P. F. and Chopra, I., "Development and Hover Testing of a Smart Trailing Edge Flap with a Piezo-Induced Bending-Torsion Coupled Actuator", American Helicopter Society National Technical Specialists' Meeting on Rotorcraft Structures, Williamsburg, Virginia, October 30-November 2, 1995.